# Strand Orientation in the DNA Quadruplex Formed from the *Oxytricha* Telomere Repeat Oligonucleotide d($G_4T_4G_4$) in Solution†

Flint W. Smith and Juli Feigon*

*Department of Chemisrty and Biochemistry and Molecular Biology Institute, University of California, Los Angeles, California 90024*

*Received February 11, 1993; Revised Manuscript Received May 20, 1993*

ABSTRACT: The structure formed from the DNA oligonucleotide d($G_4T_4G_4$) (Oxy-1.5), which contains the *Oxytricha* telomere repeat $T_4G_4$, has been investigated by two-dimensional $^1H$ and $^{31}P$ NMR spectroscopy. Sequence-specific assignments have been obtained for the $^1H$ and $^{31}P$ resonances, using a combination of methods including comparisons to the inosine- and uracil-containing derivatives d($G_4T_4G_3I$) and d($G_4UT_3G_4$). The oligonucleotide forms a symmetrical bimolecular G-quadruplex with four G-quartets and thymine loops at opposite ends of the G-quartets. Guanines are alternately *syn* and *anti* along each "strand" and all of the thymines are *anti*. The thymines loop diagonally across the G-quartet, resulting in a structure in which adjacent strands are alternately parallel and antiparallel and the glycosidic torsion angles are *syn-syn-anti-anti* around each G-quartet. There are three different types of grooves, a wide, a narrow, and two medium grooves. A diagonally looped quadruplex is formed in the presence of both $Na^+$ and $K^+$ counterions. The model structure of Oxy-1.5 is compared to the recently published crystal structure of Oxy-1.5 (Kang *et al.*, 1992), which contains many of the same features as those found in solution but differs in that the thymines loop across an edge of the G-quartet.

It has been known since the 1960s that guanosine monophosphate (GMP) (Gellert *et al.*, 1962), poly(G) (Arnott & Selsing, 1974), and poly(I) (Arnott *et al.*, 1974) can form four-stranded DNA structures [reviewed in Guschlbauer *et al.* (1990)]. Gellert (1962) proposed that these structures form by association of guanines into G-quartets in which each guanine is bonded to two neighboring guanines in a cyclic arrangement. Although the chemistry is interesting, the topic did not seem to be biologically relevant until the recent proposals that G-rich sequences found in telomeres (Oka & Thomas, 1987; Sundquist & Klug, 1989; Williamson *et al.*, 1989), immunoglobulin switch regions (Sen & Gilbert, 1988), and mutational hot spots associated with human disease (Murchie & Lilley, 1992; Smith *et al.*, 1989) may form G-quaduplex structures.

Investigations of DNA oligonucleotides containing naturally occurring G-rich sequences led to proposals for formation of two different types of G-quadruplex structures. Sen and Gilbert (1988) proposed that the unusual mobility on polyacrylamide gels of the G-rich oligonucleotides containing sequences found in immunoglobulin switch regions resulted from formation of tetrameric parallel-stranded G-quadruplexes. Sundquist and Klug (1989) proposed that the *Tetrahymena* telomere 3′ terminal overhang (TTGGGGTTGGGG) (Blackburn & Gall, 1978; Klobutcher *et al.*, 1981) dimerized by formation of guanine quartets between hairpin loops, thus forming a folded-back quadruplex structure. On the basis of gel mobility, chemical modification and footprinting, and UV cross-linking, a folded-back structure was established by Williamson *et al.* (1989) for the telomere repeat oligonucleotides of *Tetrahymena* and *Oxytricha*. The authors presented a detailed model for a unimolecular quadruplex formed from d($T_4G_4T_4G_4T_4G_4T_4G_4$), which contains four *Oxytricha* telomere repeats. The G-quadruplex core of the model was based on the fiber diffraction work of Zimmerman *et al.* (1975). Sequential tracts of guanines were modeled as all *syn* or all *anti*, resulting in a 2-fold symmetric structure with two major and two minor grooves. A similar folded quadruplex was also proposed for the oligo(dG) sequences $dG_{27}$ and $dG_{37}$ (Panyutin *et al.*, 1990). An earlier gel mobility, UV melting, and NMR study of telomere repeat oligonucleotides (Henderson *et al.*, 1987), in which G·G hairpin formation was proposed, showed NMR evidence for some *syn* and some *anti* bases in the *Tetrahymena* repeats ($T_2G_4$).

For single tracts of guanines, only the tetrameric G-quadruplexes can form; however, when there is more than one tract of guanines separated by two or more bases, it is possible that either fold-back (dimeric or unimolecular) or tetrameric G-quadruplexes might form. Sen and Gilbert (1990) proposed that the fold-back structures are excessively stabilized by $K^+$ and that the relative populations of structures depends on ionic conditions, specifically the balance of $Na^+$ and $K^+$. Evidence for multiple structures for many of these oligonucleotides was observed in these and other gel mobility studies (Williamson *et al.*, 1989; Sen & Gilbert, 1990; Hardin *et al.*, 1991; Acevedo *et al.*, 1991). Cation dependence of the formation and stability of G-quadruplexes has been observed since the early GMP studies (Chantot & Guschlbauer, 1969). The monovalent cations $Na^+$ and $K^+$ are presumed to fit into the center of or between stacked G-quartets, respectively, while cations with larger ionic radii are excluded from the center of a G-quadruplex (Guschlbauer *et al.*, 1990).

To date, the role of quadruplex formation (if any) in telomere biological function is unknown. Folding of these oligonucleotides into G-quadruplexes appears to inhibit their use as primers by telomerase, but it is suggested that G-quartet structures may act as a negative regulator of telomere elongation *in vivo* (Zahler *et al.*, 1991). The facile formation of G-quadruplexes argues for their existence and therefore a functional role *in vivo*.

† This work was supported by grants from NIH (GM37524 and GM48123) and a NSF Presidential Young Investigator Award with matching funds from AmGen Inc., Monsanto Co., and Sterling Winthrop Drug Inc. to J.F. and an NIH predoctoral training grant (GM07185) to F.W.S.

* Author to whom correspondence should be addressed.

0006-2960/93/0432-8682$04.00/0 

Several solution NMR studies of parallel tetrameric DNA and RNA quadruplexes have recently been reported. The DNA and RNA oligonucleotides d(TGGGGT) (Aboul-ela *et al.*, 1992), d(TGGGT) (Jin *et al.*, 1992), d(TTGGGG) (Wang & Patel, 1992), d(TTAGGG) (Wang & Patel, 1992), and (UGGGGU) (Cheong & Moore, 1992) tetramerize by parallel association of four strands and form G-quadruplex structures with all *anti* nucleotides. One unusual tetrameric model has been reported by Jin *et al.*, (1990) and further described by Wang *et al.* (1991a,b). The authors reported that the guanine bases in d($GGT_5GG$) and d($GGT_4CGG$) alternate 5′-*syn-anti*-3′, but they were not able to determine the strand orientation. Several calorimetric and CD studies of both parallel and foldback sequences have also been reported (Henderson *et al.*, 1987; Jin *et al.*, 1990, 1992; Balagurumoorthy *et al.*, 1992; Chen, 1992; Lu *et al.*, 1992, 1993; Weisz *et al.*, 1992).

We have been studying the structures formed by DNA oligonucleotides containing the telomeric repeat of *Oxytricha* nova $(T_4G_4)_n$, specifically, d($G_4T_4G_4$) (Oxy-1.5) and d($G_4T_4G_4T_4G_4T_4G_4$) (Oxy-3.5). These oligonucleotides contain $1^1/_2$ and $3^1/_2$ repeats of the *Oxytricha* telomere repeat sequence. We recently reported that these oligonucleotides fold to form bimolecular and unimolecular quadruplexes, respectively, in solution (Smith & Feigon, 1992). Both contain a stack of four G-quartets with alternating *syn-anti-syn-anti* nucleotides along each guanine tract and thymine loops at either end of the G-quartet stack. The Oxy-1.5 quadruplex is a symmetric structure with the thymine loops across the diagonal of the end G-quartets. Oxy-3.5 forms a related structure with four G-quartets and three thymine loops, with the first and last tract of thymines looping across the edges at one end of the quadruplex and the central thymines looping diagonally across the G-quartet at the other end. The diagonal looping of the thymines leads to several unexpected structural features. We present here the detailed NMR data, assignments, and arguments which establish the diagonally looped quadruplex structure of Oxy-1.5 in solution. The model structure of Oxy-1.5 (Smith & Feigon, 1992) is compared to the concurrently published crystal structure of Oxy-1.5 (Kang *et al.*, 1992), which contains many of the same features as those found in solution but differs in that the thymines loop along an edge of the G-quartet. A comparison of the Oxy-1.5 and Oxy-3.5 structures will be presented elsewhere (manuscript in preparation).

## MATERIALS AND METHODS

*Sample Preparation.* DNA oligonucleotides d($G_1G_2G_3G_4T_5T_6T_7T_8G_9G_{10}G_{11}G_{12}$) (Oxy-1.5) and derivatives d($G_1G_2G_3G_4T_5T_6T_7T_8G_9G_{10}G_{11}I_{12}$) (I12) and d($G_1G_2G_3G_4U_5T_6T_7T_8$-$G_9G_{10}G_{11}G_{12}$) (U5) were synthesized using an Applied Biosystems 381A synthesizer using phosphoramidite chemistry following the manufacturer's protocols. Concentrated $NH_4OH$ was used to cleave the DNA from the support and to remove blocking groups. After removal of the $NH_4OH$ by evaporation in a Speed-Vac, the DNA was redissolved in 1 mL of 2 M NaCl and ethanol-precipitated to remove small molecular weight impurities. The precipitate was redissoved in $H_2O$ and the sample was purified on a Pharmacia Sephadex G50 chromatography column eluted with $H_2O$ as previously described (Feigon *et al.*, 1992; Kintanar *et al.*, 1987). Fractions containing only full-length oligonucleotide were pooled, lyophilized, and stored desiccated until used. NMR samples were prepared by dissolving an appropriate weight of lyophilized powder in 0.4 mL of 50 mM NaCl and the pH was adjusted to 6.0 or 7.0 with NaOH. Sample concentrations were usually ~3–5 mM in strand (~1.5–2.5 mM quadruplex). The samples were dried under $N_2$ flow or by lyophilization and redissolved in 0.4 mL of 90% $H_2O$/10% $D_2O$ or 99.996% $D_2O$ (Cambridge Isotope Laboratories).

NMR samples of Oxy-1.5 with $K^+$ counterion were also prepared as described above but dissolved in 50 mM KCl, pH 6.0 (adjusted with KOH). For some samples, residual $Na^+$ or $K^+$ was removed by passage through a 1.6-X 35-cm Bio-Rad Dowex AG-50-8X cation exchange column which had been charged with $K^+$ or $Na^+$, respectively. The fractions containing the DNA were pooled, lyophilized, resuspended in 0.4 mL of $H_2O$, and transferred to a NMR tube. Samples were dried and resuspended in 90% $H_2O$ or 99.996% $D_2O$ as needed.

*NMR Spectroscopy.* NMR data was collected on a General Electric GN-500 (500 MHz $^1H$) spectrometer. One-dimensional $^1H$ spectra of samples in $D_2O$ were acquired with preirradiation of the residual HOD resonance and in $H_2O$ with a $1\bar{1}$ spin echo pulse sequence (Skelnář & Bax, 1987) over a range of temperatures from 1 to 85 °C. Phase-sensitive nuclear Overhauser effect (NOESY) spectra in $D_2O$ were acquired using the method of States *et al.* (1980) with preirradiation of the HDO peak during the recycle delay (Kumar *et al.*, 1980). NOESY spectra of Oxy-1.5 were acquired at a range of mixing times ($\tau_m$ = 35–200 ms) at temperatures of 5–50 °C. The spectral width was 8000–10 000 Hz in both dimensions in $H_2O$ and 4000–8000 Hz in $D_2O$. Between 250 and 550 $t_1$ increments of 32 acquisitions each and 2K points were collected. Between 200 and 600 complex points were processed in $t_2$ and the final zero-filled matrix size was 2K × 2K points. Phase-sensitive NOESY spectra in $H_2O$ were obtained by replacing the last 90° pulse with a $1\bar{1}$ spin echo pulse sequence and the appropriate phase cycle to suppress the large water resonance (Skelnář & Bax, 1987). The carrier was centered at the water resonance, and the delay $\tau$ was adjusted so that the excitation maximum was at ~11 ppm. Spectra in $H_2O$ were acquired at several different temperatures and mixing times. HOHAHA spectra were acquired using the MLEV17 mixing sequence and 1.5-ms trim pulses for the spin lock (Bax & Davis, 1985). The P.COSY spectrum was acquired with a flip angle mixing pulse of 90° (Marion & Bax, 1988). The $^{31}P$–$^1H$ heteronuclear COSY spectrum was acquired as described (Sklenář *et al.*, 1986).

$^{23}Na$ and $^{39}K$ NMR 1D spectra were collected using a standard one-pulse sequence with 1024 and 3500 scans, respectively. The $^{39}K$ spectra were acquired on a Bruker AM500 NMR spectrometer.

One-dimensional NMR data were processed using GEM16 software on a Nicolet 1280 computer. All 2D NMR spectra were processed using FELIX 1.1 (Hare Research) on a Silicon Graphics Iris 4D25. Two-dimensional NMR spectra were baseline-flattened with a first-order polynomial in $t_2$ and with a second-order polynomial in $t_1$. Detailed descriptions of other acquisition and processing parameters are given in the figure captions.

## RESULTS

*One-Dimensional Spectra of Oxy-1.5.* One-dimensional $^1H$ NMR spectra of Oxy-1.5 in $H_2O$ and the same sample after 24 h in $D_2O$ are shown in Figure 1. Resonance intensity corresponding to eight hydrogen-bonded imino protons (Figure 1A) and four methyl resonances (Figure 1C) are observed. The one-dimensional spectra indicate that in the conditions

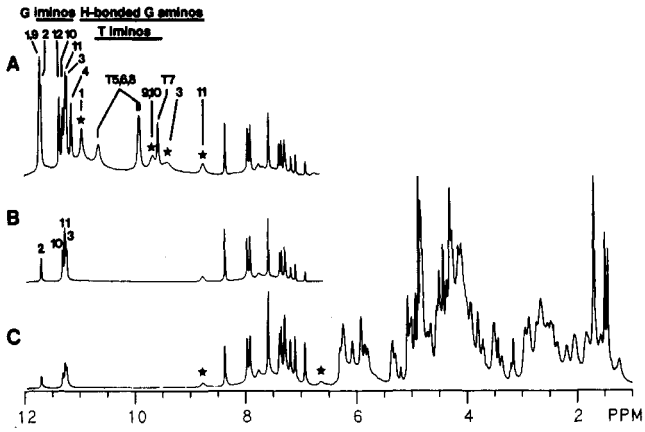


FIGURE 1: One-dimensional $^1H$ NMR spectra of Oxy-1.5 at 15 °C in (A) 90% $H_2O$ and (B and C) $D_2O$ 1 day after transfer from $H_2O$ with incubation at 25 °C. Imino and amino resonances are labeled in panel A and imino resonances still observed in $D_2O$ are labeled in panel B. Long-lived $G_{11}$ amino resonances are indicated by stars in panel C. Sample is 5.2 mM strand, 50 mM NaCl, pH 6.0. Spectra A and B were acquired with a $1\bar{1}$ spin echo pulse sequence with 8000-Hz sweep width, 128 acquisitions, 2-s recycle delay, and $\tau$ = 160 $\mu$s. Spectrum C was acquired with a standard one-pulse sequence with presaturation of HDO, 128 acquisitions, and a 2-s recycle delay. Spectra were apodized with a Gaussian multiplication of 3 Hz.

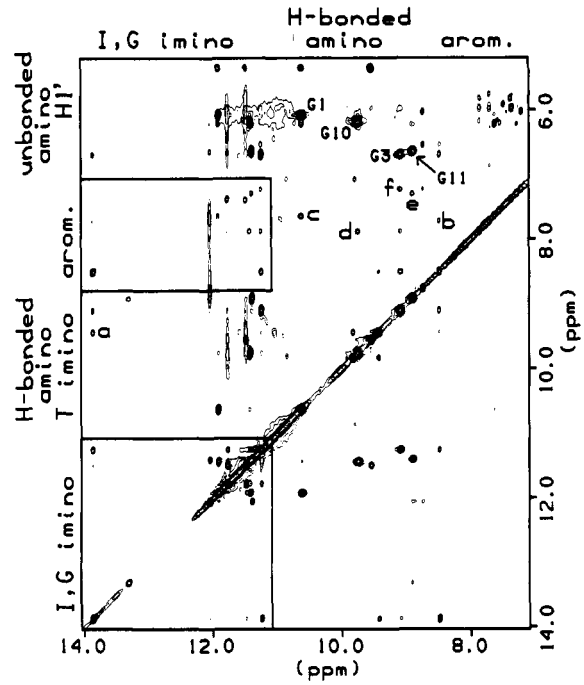


FIGURE 2: NOESY spectrum of I12 in $H_2O$ at 5 °C and $t_m$ = 200 ms. The sample is 5.6 mM strand, 50 mM NaCl, pH 6.0, 90% $H_2O$/10% $D_2O$. Boxed regions are expanded in Figure 3. Labeled NOE cross peaks are (a) I12 imino–T imino, (b) $I_{12}$H2–$G_4$H8, (c) $G_9$H8–$G_1$ amino, (d) $G_2$H8–$G_{10}$ amino, (e) $G_{10}$H8–$G_{11}$ amino and (f) $G_{11}$ amino–$G_3$ amino and hydrogen-bonded to non-hydrogen-bonded amino cross peaks of $G_1$, $G_3$, $G_{10}$, and $G_{11}$. This spectrum was acquired with 10 000-Hz spectral width in both dimensions, 2048 complex points, and 279 $t_1$ blocks of 64 acquisitions each. The residual water was subtracted with a program written by Edmond Wang utilizing a time-domain deconvolution routine (Marion *et al.*, 1989). The spectrum was zero-filled to 2048 complex points in $t_1$ and the data were apodized with a 70° skewed sine squared in $t_2$ (500 points, 1.1 skew) and $t_1$ (280 points, 1.1 skew).

used here Oxy-1.5 forms primarily a single well-defined structure with hydrogen-bonded bases. Since resonances from only one strand are observed, if the structure has more than one strand it must be symmetric.

An unusual feature of the structure formed by Oxy-1.5 is the relatively very slow exchange rate of the exchangeable imino and amino resonances. All of the imino resonances can be observed in $H_2O$ up to 65 °C (not shown). Four of the imino resonances are observed in the sample 1 day after transfer to $D_2O$ (Figure 1B,C) and are still present after more than 14 days (Smith & Feigon, 1992). In addition, two pairs of amino proton resonances ($G_{11}$ and $G_3$) are also unusually slowly exchanging; both $G_{11}$ amino proton resonances can still be observed after transfer of the sample from $H_2O$ to $D_2O$ (Figure 1C).

*NOESY Spectra in $H_2O$—Evidence for G-Quartets.* NOESY spectra in $H_2O$ of Oxy-1.5 and I12 [d(GGGGTTTTGGGI)] show strong intranucleotide NOE cross peaks between each of the G imino resonances and a pair of G amino resonances and a weak internucleotide cross peak to an H8 resonance, as expected for G-quartet hydrogen bonding (Smith & Feigon, 1992). A portion of a NOESY spectrum in $H_2O$ of I12 is shown in Figure 2. The hydrogen-bonded imino proton of $I_{12}$ is readily identified because it resonates at much lower field than the G imino protons. Most of the amino protons of Oxy-1.5 and I12 give rise to well-resolved pairs of resonances, rather than the single broad resonance from the hydrogen-bonded and non-hydrogen-bonded amino protons usually observed in B-DNA (Boelens *et al.*, 1985). NOE cross peaks between the hydrogen-bonded (lower field) and non-hydrogen-bonded (higher field) amino resonances of four of the G nucleotides are labeled on Figure 2.

NOE cross peaks between the imino and GH8 resonances are identified in the expanded portion of Figure 2 shown in Figure 3A. These weak cross peaks are consistent with the hydrogen bonding proposed for G-quartets, in which the N1 imino and N2 amino of one guanine are hydrogen-bonded to the C6 carbonyl and N7, respectively, of another guanine. Direct NOE cross peaks between the G amino and GH8 proton resonances of each base pair in each G-quartet are also expected. These are observed for the more slowly exchanging G aminos and are labeled on Figure 2 (peaks c–f). Further evidence of the base pairing expected for guanines in a G-quartet is obtained for I12 from the NOE cross peak observed between $I_{12}$H2 and $G_4$H8 (Figure 2, peak b).

Although the pattern of NOE cross peaks observed in the NOESY spectra in $H_2O$ is only consistent with the hydrogen bonding expected for G-quartets, the sequence-specific assignment of the imino proton resonances could only be obtained after the base proton resonances were assigned. The assignments of the exchangeable resonances are therefore discussed after the nonexchangeable resonance assignments.

*Assignments of Sugar Spin Systems.* Assignments of the sugar spin systems were obtained primarily by analysis of P.COSY and HOHAHA spectra (not shown) using standard methods (Wüthrich, 1982). All of the 1′,2′,2″, and 3′, and some of the 4′ and 5′,5″ resonances in a given sugar were identified from these spectra. Some of the H3′–H4′ cross peaks were not observed in the P.COSY and HOHAHA spectra due to small $J$-coupling constants. Therefore, sugar proton cross peaks in the NOESY spectra in $D_2O$ (Figure 4, box D) were used to complete the assignment of the 4′ and 5′,5″ resonances. The 2′ and 2″ resonances were stereospecifically assigned on the basis of the H1′–H2′ and H1′–H2″ NOE cross-peak intensities in a short mixing time NOESY spectrum (not shown). Regardless of the sugar conformation, the H1′–H2″ interproton distance is always shorter than the H1′–H2′ distance. In B-DNA, the H2′ resonance of a given sugar almost always occurs upfield of the H2″ resonance

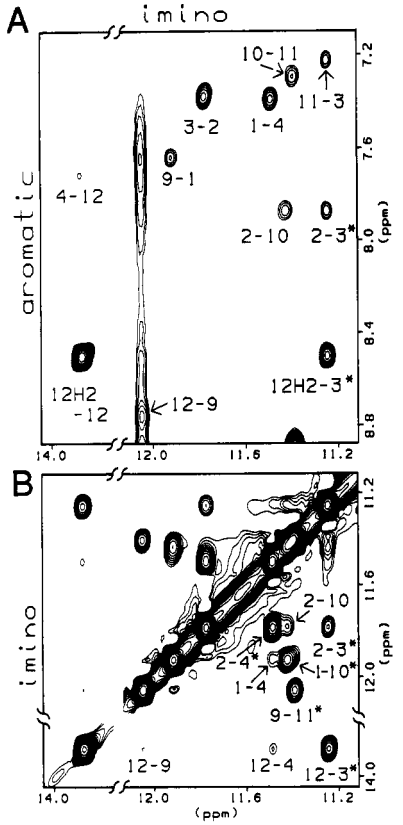


FIGURE 3: Expanded regions of the NOESY spectrum of I12 in $H_2O$ in Figure 2 showing (A) imino–aromatic, amino cross peaks and (B) imino–imino cross peaks. Interquartet NOE cross peaks are indicated by asterisks. In panel A, H8–imino cross peaks are labeled, e.g., $G_4$H8–$I_{12}$ imino. Intraquartet connectivities are seen around each G-quartet, i.e., from $G_1$ to $G_4$ to $I_{12}$ to $G_9$ and back to $G_1$ for the end G-quartets and $G_2$ to $G_{10}$ to $G_{11}$ to $G_3$ and back to $G_2$ for the central G-quartets. The large vertical streak is the NOE from $G_9$ imino to the broad resonances of the $G_9$ amino protons.

(Altona, 1982). However, in Oxy-1.5 this rule does not hold. The H2′ resonances of nucleotides 3, 6, 9, 10, 11, and 12 are *downfield* of their H2″ resonances. The 5′,5″ pairs were not stereospecifically assigned.

*NOESY Spectra of Oxy-1.5 in $D_2O$—Glycosidic Torsion Angles, Loop Orientation, and Sequence-Specific Assignments of Nonexchangeable Resonances.* A NOESY spectrum of Oxy-1.5 in $D_2O$ is shown in Figure 4. The base–base, base–H1′, and base–methyl regions of the spectrum (boxes A–C) used for sequential assignments of B-DNA are shown expanded in Figure 5. In the base–H1′ region (Figure 5B), four *syn* G nucleotides are identified by the intense H8–H1′ NOE cross peaks. All of the remaining G and T nucleotides have the smaller intranucleotide base–H1′ cross peaks normally observed for the *anti* conformation.

Because of the *syn* nucleotides, normal sequential connectivities (Feigon *et al.*, 1983; Hare *et al.*, 1983; Scheek *et al.*, 1983; Wüthrich 1986) are not observed for this molecule (Feigon *et al.*, 1992; Smith & Feigon, 1992). Instead, for the guanines sequential base–H1′ connectivities are only observed between each *syn* guanine and the adjacent 3′-*anti* guanine. There are four nonequivalent 5′-*syn-anti*-3′ guanine pairs. The inter- and intranucleotide H8–H1′ NOEs observed for each set are indicated by the lines which form boxes in Figure 5B. A sequential H8–H8 NOE is also observed for each pair of 5′-*syn-anti*-3′ guanines (Figure 5A). In contrast to the numerous sequential NOE connectivities between 5′-*syn-anti*-3′ guanine residues, there are almost no 5′-*anti-syn*-3′ connectivities, since the *syn* orientation of the base places the

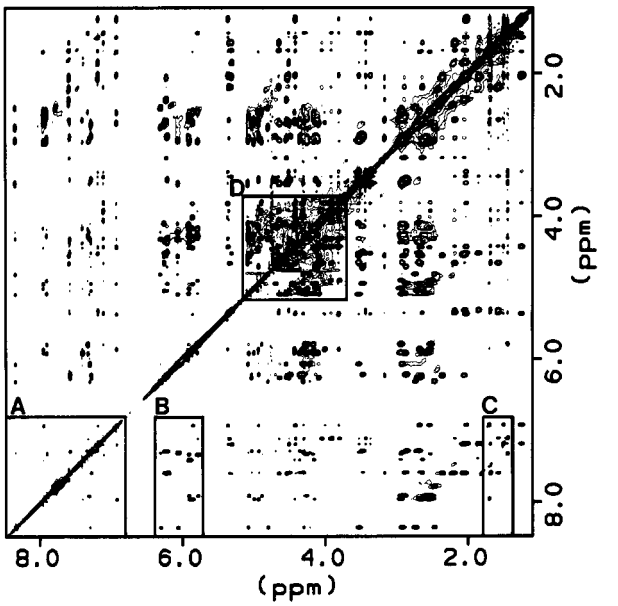


FIGURE 4: NOESY spectrum of Oxy-1.5 in $D_2O$ at 25 °C and $\tau_m$ = 200 ms. The sample is the same as in Figure 1. Boxed regions A, B, and C are expanded in Figure 5. The spectrum was acquired with an 8000-Hz spectral width in both dimensions, but only the central 4000 Hz was processed into a final 2K × 2K points matrix. Five hundred fifty $t_1$ blocks were collected with 32 acquisitions each. The spectrum was apodized using a 75° shifted skewed sine squared function in $t_2$ (600 points, 1.1 skew) and $t_1$ (550 points, 1.1 skew).

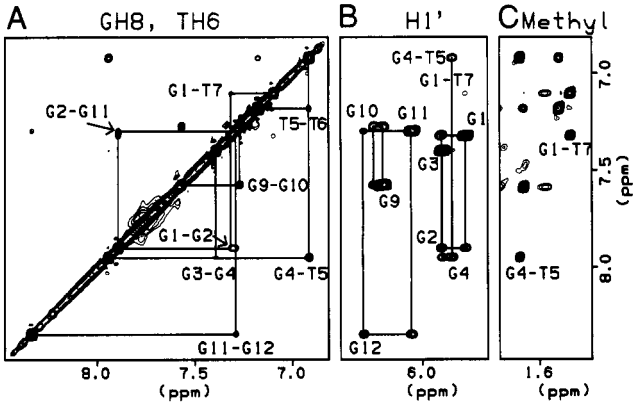


FIGURE 5: Expanded regions of NOESY spectrum in Figure 4 containing the (A) aromatic–aromatic, (B) aromatic–H1′, and (C) aromatic–methyl cross peaks. In panel A, the sequential GH8–GH8 NOE cross peaks are labeled below the diagonal and the nonsequential $G_1$H8–$T_7$H6 and $G_2$H8–$G_{11}$H8 NOE cross peaks are labeled above the diagonal. In panel B, sequential connectivities between *syn–anti* G pairs are indicated by connected rectangles. The intense H8–H1′ cross peaks for $G_1$, $G_3$, $G_9$, and $G_{11}$ indicate that these nucleotides are *syn*. In panel C, cross peaks from $G_4$H8–$T_5$Me and $G_1$H8–$T_7$Me are labeled.

H8 proton greater than 6 Å away from the H8 the most of the sugar protons on the neighboring 5′ nucleotide. The only 5′-*anti-syn*-3′ sequential connectivities are weak sequential $G_{2n}$H3′–$G_{2n+1}$H1′ or weak to medium $G_{2n}$H1′–$G_{2n+1}$H4′,5′,5″ cross peaks. Thus, although it was relatively easy to identify four sets of *syn-anti* sequential guanines in the structure formed by Oxy-1.5, which indicate that the guanines are *syn-anti-syn-anti* along the strand, the *ordering* of these *syn-anti* guanine pairs and thus the sequence-specific assignments of the guanines from the NOESY spectra were not straightforward.

There are NOE cross peaks between resonances from one guanine in each 5′-*syn-anti*-3′ pair and the thymines. Some of these are labeled in Figure 2 (peak a) and Figure 5.

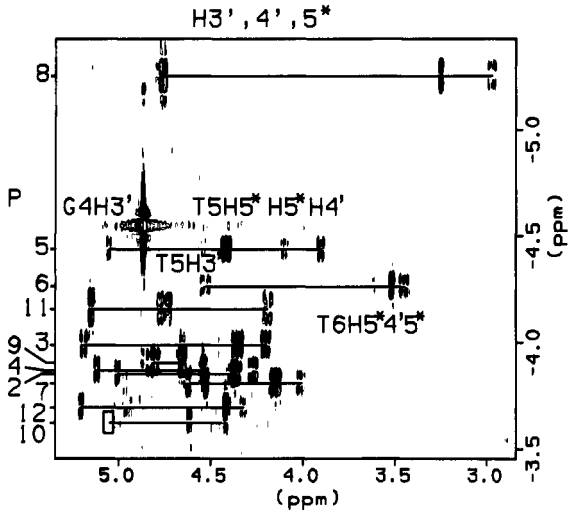


FIGURE 6: $^{1}H$–$^{31}P$ heteronuclear COSY of Oxy-1.5 at 25 °C. Sample is the same as in Figure 1. Phosphate assignments are indicated on the side of the spectrum. Connectivities to the 5′H3′ and 3′H4′,-H5′,H5″ resonances are indicated by solid lines and are labeled for $T_5$ and $T_6$ phosphates. The box indicates the missing $G_9H3'$–$G_{10}P$ cross peak. The spectrum was acquired with a spectral width of 1400 Hz for the $^{1}H$ dimension and 500 Hz for the $^{31}P$ dimension. Fifty $t_1$ blocks of 128 acquisitions each were collected. Four hundred complex points were processed in $t_2$ and 50 increments were processed in $t_1$. The spectrum was zero-filled to 1K × 1K complex points and processed with a 30° shifted sine-squared apodization window (skew 0.7) in both dimensions.

Additional guanine–thymine cross peaks were observed in the base–H2′,H2′ region of the NOESY spectra. The only symmetric quadruplexes in which four nonequivalent guanines can be near thymines are dimeric quadruplexes in which the thymine tracts form loops at opposite ends (see Discussion).

The establishment of a dimeric G-quadruplex structure with thymine loops at opposite ends places limitations on the order (*i.e.*, assignment) of the guanine *syn-anti* pairs. There are cross peaks between two *syn* Gs and two *anti* Gs to thymines. Sequential connectivities between an *anti* G and a T identified $G_4$ and thus $G_3$. The only other *anti* G which could have (nonsequential) cross peaks to the thymines is $G_{12}$, which allowed assignment of $G_{12}$ and thus $G_{11}$. This left only the $G_1$-$G_2$ and $G_9$-$G_{10}$ pairs unassigned. There is an additional H8–H8 cross peak between an *anti* G and $G_{11}$ (Figure 5A and, for I12, Figure 7). This $G_{syn}H8$–$G_{anti}H8$ cross peak is between two guanines which are not a 5′-*syn-anti*-3′ pair. As discussed in detail in the Discussion, this type of *syn-anti* cross peak is only predicted by a diagonally looped quadruplex structure. Using this model, we were able to assign the NOE cross peak as $G_{11}H8$–$G_2H8$. With $G_2H8$ identified, we had the assignments for $G_1$ and G2, and by elimination $G_9$ and $G_{10}$. Thymines 5 and 6 we identified by sequential connectivities from $G_4$-$T_5$-$T_6$ (all *anti*) (Figure 5). $T_7$ and $T_8$ were tentatively assigned from NOE cross peaks.

The self-consistent assignments obtained from the NOESY spectra were used in generating the diagonally looped structure of Oxy-1.5 (Smith & Feigon, 1992) and have therefore been presented here in detail. These assignments were subsequently confirmed by analysis of $^{31}P$–$^{1}H$ heteroCOSY spectrum as well as by spectra obtained on uracil- and inosine-substituted derivatives.

*Sequence-Specific Assignments by $^{31}P$–$^{1}H$ HeteroCOSY.* A $^{31}P$–$^{1}H$ heteroCOSY spectrum is shown in Figure 6. Since the H3′, H4′, and H5′,H5″ resonances in each sugar had been identified, this spectrum provided direct model-independent sequential assignments of Oxy-1.5. Assignments of the phosphate resonances are indicated along the side of the spectrum. Each phosphorous resonance has cross peaks to H4′,H5′,H5″ of the 3′ nucleotide and to the H3′ of the 5′ nucleotide. Thus, sequential connectivities can be traced along the DNA strand without any structural assumptions (Pardi *et al.*, 1983). The $G_9H3'$–$G_{10}P$ cross peak is not observed, leading to a break in the sequential connectivities. Other than this one gap, each H3′ can be traced to the sequential H4′ or H5′,5″, allowing the assignment of all 12 sugars. All of the assignments previously reported (Smith & Feigon, 1992) were confirmed by this spectrum, including the tentative assignments of the T nucleotide resonances. Assignments of the proton and phosphorus resonances of Oxy-1.5 are given in Table I.

*NOESY Spectra of Inosine- and Uracil-Substituted Derivatives in $D_2O$.* The assignments of nonexchangeable resonances were also confirmed by analysis of the spectra obtained for Oxy-1.5 derivatives containing inosine or uracil substitutions for guanine or thymine, respectively. The U5 and I12 derivatives gave spectra which were essentially identical to those observed for Oxy-1.5 except in the region of the substituted nucleotide, indicating that they form essentially the same structures (*e.g.*, compare Figure 5A and 7 and Table I and II). The U5 [d(GGGGUTTTGGGG)] derivative confirms assignments of $T_5$ and $G_4H8$. The unique $U_5H5$ resonance unambiguously identifies the substitution. Sequential NOE cross peaks from $G_4$ to $U_5$ confirms the identification of $G_4H8$ (spectrum not shown). In the NOESY spectrum of I12 the unique $I_{12}H2$ resonance has an NOE cross peak to $G_4H8$ (Figure 7 and Figure 2, peak b). Thus, $I_{12}$ and $G_4$ are neighbors within a G-quartet.

The I12 derivative gave the best-resolved spectra of all of the molecules investigated. Spectra of I12 were therefore used to confirm many of the cross-peak assignments and to determine cross-peak intensities of peaks that overlap in the spectra of Oxy-1.5. Several of the important base–base cross peaks are indicated in Figure 7. Sequential GH8–GH8 cross peaks are indicated below the diagonal, while the nonsequential $G_2H8$–$G_{11}H8$ and other cross peaks are indicated above the diagonal. Sequence-specific assignments of I12 are given in Table II. The sequential NOE connectivities observed for Oxy-1.5 and I12 are summarized in Figure 8.

*Assignments of the Exchangeable Resonances of Oxy-1.5.* In the imino–imino region of the NOESY spectrum of I12 in $H_2O$ (Figure 3B), many cross peaks are observed between the eight imino proton resonances. In DNA duplexes, imino–imino cross peaks can be used to make sequential assignments along the strand (Boelens *et al.*, 1985). This was not possible for Oxy-1.5, since it could not be known *a priori* which imino–imino distances would be the shortest. Assignments of the imino and amino resonances were therefore made using cross peaks from the previously assigned H8 resonances. The intra- and interquartet imino–H8 NOE cross peaks are identified in Figure 3A. Once the G-quartet bonding was established, assignments could be made on the basis of cross peaks between assigned H8 resonances and amino and imino protons. These assignments are dependent on the model used being correct, because the exchangeable resonances are assigned from the neighboring (base-paired) guanine. However, we have two independent checks on these assignments. The $I_{12}$ imino resonance in I12 is unambiguously identified by its unique chemical shift and NOE cross peak to the IH2. A second check is the internal consistency of the imino–imino NOE cross peaks assigned using the various models. Attempts to assign the imino resonances assuming the edge-looped models

Table I: Assignments of the $^1H$ and $^{31}P$ Resonances of Oxy-1.5 at 25 °C in 50 mM NaCl, pH 6.0[a]

| | imino[b] | amino (2)[b] | amino (1)[b] | H8,H6 | H1′ | H3′ | H4′ | H5′,5″ | H2″ | H2′ | methyl | phos |
|---|---|---|---|---|---|---|---|---|---|---|---|---|
| $G_1$ | 11.75 | 10.99 | 6.06 | 7.32 | 5.78 | 4.89 | 4.30 | 3.92, 3.79 | 2.94 | 2.52 | | |
| $G_2$ | 11.69 | na[c] | na | 7.89 | 5.90 | 5.07 | 4.26 | 4.26, 4.16 | 2.88 | 2.59 | | −3.85 |
| $G_3$ | 11.25 | 9.39 | 6.56 | 7.39 | 5.91 | 5.00 | 4.36 | 4.25, 4.10 | 2.64 | 2.95 | | −3.99 |
| $G_4$ | 11.17 | 9.96 | 5.87 | 7.94 | 5.85 | 4.93 | 4.43 | 4.15, 4.14 | 2.68 | 2.53 | | −3.87 |
| $T_5$ | na | | | 6.91 | 5.36 | 4.42 | 3.81 | 4.30, 4.00 | 2.02 | 1.25 | 1.70 | −4.44 |
| $T_6$ | na | | | 7.18 | 5.30 | 4.50 | 3.43 | 3.53, 3.36 | 1.85 | 2.04 | 1.50 | −4.26 |
| $T_7$ | 9.58 | | | 7.10 | 5.34 | 4.64 | 4.41 | 4.05, 3.91 | 2.18 | 1.57 | 1.44 | −3.81 |
| $T_8$ | na | | | 7.58 | 6.22 | 4.54 | 3.17 | 2.89, 2.64 | 2.36 | 2.05 | 1.68 | −5.25 |
| $G_9$ | 11.73 | 9.65 | 7.51 | 7.57 | 6.20 | 4.93 | 4.47 | 4.69, 4.13 | 2.86 | 3.47 | | −3.91 |
| $G_{10}$ | 11.31 | 9.71 | 6.30 | 7.27 | 6.25 | 5.03 | 4.50 | 4.36, 4.31 | 2.69 | 2.71 | | −3.63 |
| $G_{11}$ | 11.26 | 8.76 | 6.68 | 7.29 | 6.06 | 5.08 | 4.56 | 4.64, 4.08 | 2.92 | 3.53 | | −4.16 |
| $G_{12}$ | 11.37 | na | na | 8.34 | 6.30 | 4.80 | na[d] | 4.30[d], 4.21[d] | 2.47 | 2.74 | | −3.70 |

[a] Chemical shifts are given in parts per million. [b] Chemical shift at 5 °C. [c] na, not assigned. [d] 4′, 5′, 5″ ambiguous.

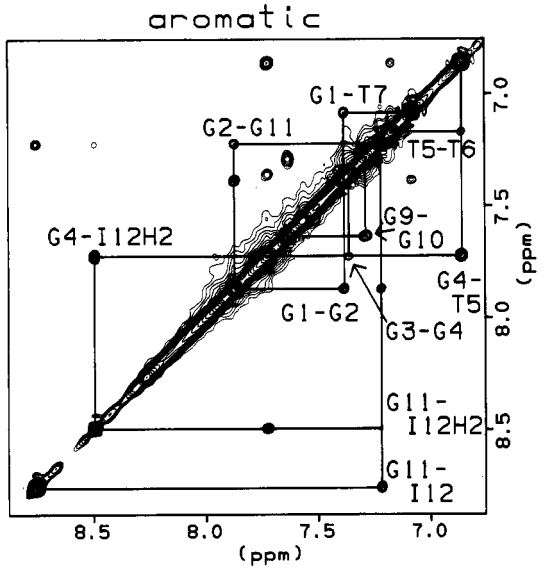


FIGURE 7: Portion of a NOESY spectrum of I12 in $D_2O$ at 5 °C and $\tau_m$ = 200 ms showing the region containing the aromatic resonances and cross peaks. The sample is the same as Figure 2 after transfer to $D_2O$. The sequential GH8–GH8 NOE cross peaks are labeled below the diagonal and the nonsequential NOE cross peaks are labeled above the diagonal. The spectrum was acquired with a spectral width of 4405 Hz in both dimensions and 256 $t_1$ blocks of 32 acquisitions each and 1024 complex points. The spectrum was zero-filled to 2K × 2K complex points and apodized with an 80° shifted skewed sine squared function in both dimensions (257 points, 1.1 skew).

gave inconsistent results; *i.e.*, predicted imino–imino NOEs were absent and unexpected NOEs were present.

*Deoxyribose Sugar Conformation.* The P.COSY spectrum was used to evaluate the sugar conformations in Oxy-1.5. The H1′–H2′,H2″ cross peaks were simulated using the CHEOPS software (Macaya *et al.*, 1992; Schultze and Feigon, in preparation) in order to obtain coupling constants for the deoxyribose sugar protons in Oxy-1.5. The coupling constants were analyzed using the PSEUROT software (de Leeuw & Altona, 1983) to determine the percentage of S- or N-type sugars. All of the sugars are predominantly S-type, as indicated in Table III.

*Other Possible Conformations of Oxy-1.5 in $Na^+$.* The samples of Oxy-1.5 and derivatives used for the structural studies described here were prepared by dissolving the purified, lyophilized DNA in 50 mM NaCl and adjusting the pH. Spectra of these samples often show, in addition to the predominant resonances corresponding to the structure described in this paper, some underlying broad resonances that we attribute to possible formation of some tetrameric quadruplexes or aggregated structures. There is also evidence for some other structures which give rise to some small resonances and cross peaks. These alternative conformations could be largely eliminated by one or more cycles of heating the sample to 93 °C, followed by slow cooling. The amount of alternative conformations present in the samples seems to be subtly dependent on exactly how the sample was prepared. For some samples, *e.g.*, the Oxy-1.5 spectra presented here, the spectra from the initially dissolved sample indicated the presence of only the single structure discussed here and no heating/cooling was required.

*Effect of $Na^+$ and $K^+$ Cations on Oxy-1.5 Structure.* NMR samples of Oxy-1.5 were also prepared in 50 mM KCl. The one-dimensional spectra (not shown) of these samples had the same general features of the samples in 50 mM NaCl but different chemical shifts for many of the resonances. However, two-dimensional spectra (not shown) of the 50 mM KCl samples gave assignments that were only consistent with the formation of the same type of diagonally looped quadruplex as that found for Oxy-1.5 in 50 mM NaCl. The NOE intensities are qualitatively the same for the G-tracts, but there are some substantial differences in the NOE cross-peak intensities in the thymine loops, especially for $T_8$. Thus, samples of Oxy-1.5 in 50 mM NaCl and 50 mM KCl form qualitatively the same structure.

Some of the NMR samples prepared in 50 mM NaCl gave one- and two-dimensional NMR spectra that were like those of the samples prepared in 50 mM KCl. One of these was the sample used for our previously published spectra of Oxy-1.5 (Smith & Feigon, 1992), for which a diagonally looped structure was obtained. The two different types of spectra for DNA samples dissolved in 50 mM NaCl were extremely puzzling to us for a long time. One-dimensional $^{39}K$ NMR spectra of these samples finally revealed that they contained 5–15 mM $K^+$. This $K^+$ is apparently acquired during the purification process and must be picked up as a minor impurity which binds tightly to Oxy-1.5 and therefore is effectively concentrated on the DNA. The $K^+$ can be removed by passage of the sample over a cation-exchange column without denaturing the DNA. Resulting spectra of the DNA dissolved in NaCl are the same as those presented in this paper. The $Na^+$ in samples prepared in NaCl can also be exchanged to $K^+$ (as judged by $^{23}Na$ NMR) by cation-exchange chromatography.

In recent studies, we have found that the structures of Oxy-1.5 in NaCl and KCl are in intermediate exchange on the NMR time scale and that addition of only a few millimolar KCl to a 50 mM NaCl sample shifts the equilibrium toward the KCl-only conformation. These studies will be presented elsewhere (manuscript in preparation).

Table II: Assignments of the $^1$H Resonances of I12 at 25 °C in 50 mM NaCl, pH 6.0[a]

| | imino[b] | amino (2)[b] | amino (1)[b] | H8,H6 | H1′ | H3′ | H4′ | H5′,5″ | H2″ | H2′ | methyl |
|---|---|---|---|---|---|---|---|---|---|---|---|
| $G_1$ | 11.91 | 10.62 | 6.08 | 7.35 | 5.82 | 4.89 | 4.31 | 3.91, 3.81 | 2.97 | 2.59 | |
| $G_2$ | 11.78 | 9.79[c] | 6.10[c] | 7.84 | 5.97 | 5.05 | 4.26 | 4.26, 4.18 | 2.85 | 2.53 | |
| $G_3$ | 11.25 | 9.09 | 6.69 | 7.39 | 5.96 | 5.03 | 4.42 | 4.25, 4.08 | 2.83 | 3.24 | |
| $G_4$ | 11.49 | 9.43[c] | 6.05[c] | 7.71 | 5.79 | 4.94 | 4.39 | 4.17, 4.17 | 2.59 | 2.51 | |
| $T_5$ | na[d] | | | 6.86 | 5.35 | 4.42 | 3.79 | 4.31, 3.98 | 1.98 | 1.18 | 1.65 |
| $T_6$ | na | | | 7.17 | 5.28 | 4.50 | 3.44 | 3.50, 3.34 | 1.83 | 2.06 | 1.49 |
| $T_7$ | 9.54 | | | 7.08 | 5.36 | 4.65 | 4.41 | 4.05, 3.92 | 2.20 | 1.55 | 1.43 |
| $T_8$ | na | | | 7.58 | 6.20 | 4.53 | 3.15 | 2.89, 2.65 | 2.36 | 2.04 | 1.70 |
| $G_9$ | 12.05 | 8.88[c] | 7.67[c] | 7.62 | 6.22 | 4.92 | 4.47 | 4.69, 4.13 | 2.88 | 3.44 | |
| $G_{10}$ | 11.43 | 9.75 | 6.18 | 7.31 | 6.23 | 5.01 | 4.50 | 4.36, 4.31 | 2.66 | 2.66 | |
| $G_{11}$ | 11.39 | 8.90 | 6.64 | 7.22 | 6.02 | 5.08 | 4.56 | 4.61, 4.09 | 2.90 | 3.50 | |
| $I_{12}$ | 13.87 | 8.52[e] | | 8.71 | 6.56 | 4.85 | na[f] | 4.34[f], 4.24[f] | 2.57 | 2.82 | |

[a] Chemical shifts are given in parts per million. [b] Chemical shifts at 5 °C. [c] Approximate value (broad peak). [d] na, not assigned. [e] Inosine H2. [f] 4′, 5′, 5″ ambiguous.

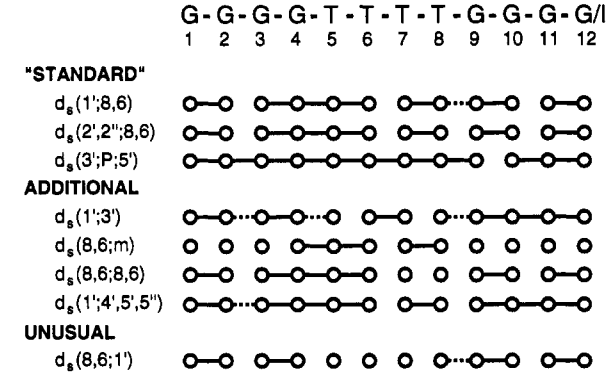


FIGURE 8: Summary of sequential NOE connectivities observed in Oxy-1.5 and I12.

Table III: Coupling Constants of Deoxyribose Protons and Calculated Percent S Sugar Conformations of Oxy-1.5 at 25 °C in 50 mM NaCl, pH 6.0[a]

| | H1′–H2′ | H1′–H2″ | H2′–H2″ | H2′–H3′ | H2″–H3″ | % S |
|---|---|---|---|---|---|---|
| $G_1$ | 10.9 | 3.7 | −14.5 | 4.6 | 4.1 | 85 |
| $G_2$ | 11.5 | 4.8 | −14.2 | 6.2 | 2.1 | 91 |
| $G_3$ | 10.1 | 5.0 | −13.3 | 5.7 | 1.0 | 93 |
| $G_4$ | 11.6 | 3.1 | −12.8 | 3.3 | 2.0 | 99 |
| $T_5$ | 6.7 | 7.7 | −15.6 | 9.5 | 1.1 | 73 |
| $T_6$ | 11.6 | 4.8 | −14.2 | 5.6 | 1.0 | 100 |
| $T_7$ | 7.3 | 5.5 | −15.0 | 5.7 | 2.4 | 74 |
| $T_8$ | 9.1 | 5.0 | −14.1 | 5.6 | 1.1 | 89 |
| $G_9$ | 11.1 | 3.8 | −14.2 | 2.7 | 3.5 | 93 |
| $G_{10}$ | 10.4 | 3.7 | −14.3 | 5.4 | 0.8 | 100 |
| $G_{11}$ | 10.2 | 5.0 | −14.1 | 3.1 | 1.0 | 99 |
| $G_{12}$ | 9.9 | 5.9 | −14.0 | 5.8 | 1.0 | 86 |

[a] Coupling constants are given in hertz.

## DISCUSSION

*Oxy-1.5 Forms a Symmetrical Quadruplex in Solution.* The one-dimensional $^1$H NMR spectra of Oxy-1.5 show eight hydrogen-bonded G-imino resonances and four thymine methyl resonances (Figure 1). Although a unimolecular hairpin model with G·G base pairs hydrogen-bonded via both iminos can be constructed, such a structure could not also have the hydrogen-bonded amino protons which are evident from the NOESY spectra in water (Figure 2). Other types of G·G pairing, *e.g.*, the G·G pairing proposed for purine·purine·pyrimidine triplexes (Radhakrishnan *et al.*, 1991), are also not consistent with the NMR data. The G imino–amino–H8 cross peaks which are observed in the NOESY spectra in water are consistent only with the type of bonding proposed for G-quartets. We note that this type of base pairing alone is not proof of G-quartet formation. In model structures in which all guanine nucleotides in a given tract have a single conformation, *i.e.*, all *syn* or all *anti*, the bases could potentially form a hydrogen-bonded spiral. Such structures have been previously proposed for GMP (Gellert *et al.*, 1962). However, in structures such as the one observed here in which the bases alternate glycosidic torsion angles *syn* and *anti* along the strand, such a spiral could not form. Strong evidence for G-quartets is seen in the cyclic NOEs from H8 to imino observed around each G-quartet (Figure 3A). We trace from $G_1$ to $G_4$ to $I_{12}$ to $G_9$ and back to $G_1$ and from $G_2$ to $G_{10}$ to $G_{11}$ to $G_3$ and back to $G_2$. Thus, the guanines must be hydrogen-bonded in quartets as proposed.

A quadruplex structure requires at least four tracts of guanines. Since a single Oxy-1.5 oligonucleotide contains only two guanine tracts, two or four strands must associate to form a quadruplex. Resonances for only one strand are observed (*e.g.*, there are only eight G imino and four T methyl resonances), indicating that the quadruplex must be symmetrical. On the basis of these considerations alone, the Oxy-1.5 structure could only be either a symmetric dimer or a symmetric tetramer, composed of four or eight G-quartets, respectively.

*Oxy-1.5 Forms a Dimer with Thymine Loops at Opposite Ends of the Quadruplex.* The presence of NOEs between thymines and more than two nonequivalent guanines (Figures 2 and 4–6) unambiguously identifies the quadruplex structure as a dimer with loops at opposed ends, even without sequence-specific assignments. In all symmetric tetrameric quadruplexes, only two nonequivalent guanines ($G_9$ and $G_4$) can be adjacent to thymines. This is also true for the dimeric quadruplexes with both loops at one end (Figure 9). One other symmetric quadruplex, the "crown" model in which the thymines loop from one end of the stack of G-quartets to the other end rather than across the face of an end G-quartet, has been proposed for coherence of *Oxytricha* telomeres (Acevedo *et al.*, 1991). The NOE connectivities from thymines (5, 7, and 8) to guanines 1, 4, 9, and 12 but not to guanines 2, 3, 10, or 11, are inconsistent with this model. This leaves only four dimeric quadruplexes with the required (observed) 2-fold symmetry, illustrated in Figure 10. Two of these are diagonally looped models (Figure 10A,B), one has the loops across wide grooves [as observed in the crystal structure (Kang *et al.*, 1992)] (Figure 10C), and one has loops across the narrow grooves (Figure 10D). Note that all of the quadruplexes in Figure 10 have only two nonequivalent G-quartets, consistent with the NMR data, while the symmetric quadruplexes have either eight (Figure 9A) or four (Figure 9B–D) nonequivalent G-quartets. The quadruplexes illustrated in Figure 10 also are the only symmetric quadruplexes in which the 5′ and 3′ ends ($G_1$ and $G_{12}$) are near thymines.

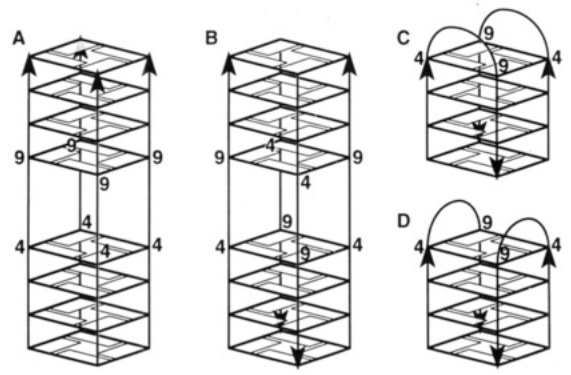

FIGURE 9: Orthographic schematics of the symmetric quadruplex structures eliminated by the observation of NOE connectivities between more than two guanines and thymines: (A) parallel tetramer, (B) antiparallel tetramer, (C) dimer with both loops at one end across the wide grooves, and (D) dimer with both loops at one end across the narrow grooves. In all of these structures, only $G_4$ and $G_9$ are near thymines.

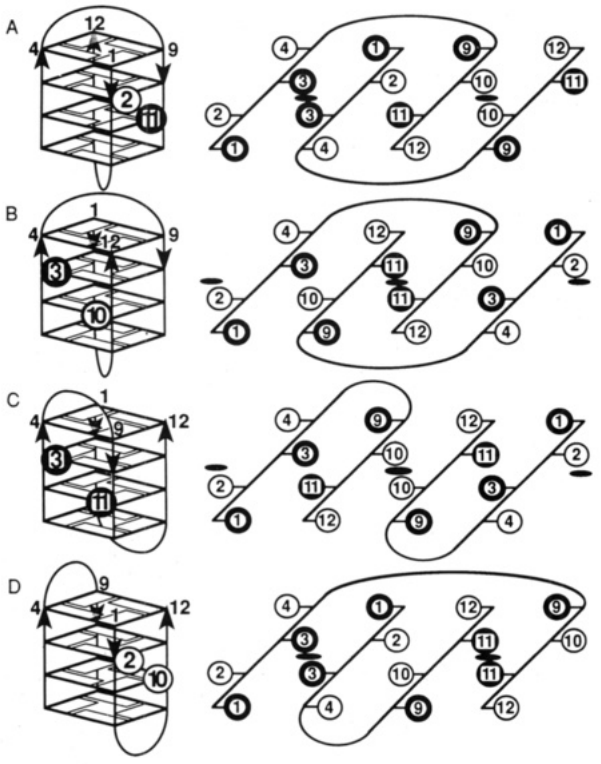

FIGURE 10: Orthographic (left) and unrolled surface map (right) schematics of the four possible symmetric quadruplex structures with loops at opposite ends and bases alternating *syn-anti-syn-anti* along each strand which could potentially be formed by Oxy-1.5: (A) diagonally looped structure consistent with the NMR data on Oxy-1.5 presented here, (B) the other possible diagonally looped structure, (C) edge-looped structure with loops that span the wide groove (Kang *et al.*, 1992), and (D) edge-looped structure with loops that span the narrow groove. The locations of GH8 protons are indicated by bold circles (*syn* base) and thin circles (*anti* base). Only the long-range GH8–GH8 interaction expected for each possible structure is shown on the orthographic schematics. Bold elongated ovals in the unrolled surface map schematics indicate symmetry axes.

*Guanines Are 5′-syn-anti-syn-anti-3′ along Each Edge of the Quadruplex.* The base pairing in a G-quartet requires that a change of strand direction requires a change in nucleotide conformation from *anti* to *syn* or vice versa (assuming a regular backbone conformation). Thus, simple models proposed for antiparallel (or fold-back) G-quadruplex structures had nucleotides that were alternately all *syn* and all *anti* in each tract of guanines (Williamson *et al.*, 1989), although the possibilities for other conformations were noted (Sundquist & Klug, 1989). [One model proposed by Guschlbauer *et al.* (1990) for d[$(T_4G_4)_4$] is alternating *anti-syn* along the guanine tracts but is physically impossible because the base orientation precludes G-quartet formation.] In contrast to the simple models, the nucleotides along each edge of the quadruplex formed by Oxy-1.5 are alternately *syn-anti* starting with a 5′-*syn* nucleotide. The *syn-anti* alternation has been observed for several G-quadruplexes formed from oligonucleotides with tracts of guanines on either side of two or more pyrimidines (Smith & Feigon, 1991, 1992; Wang *et al.*, 1991a,b, 1993; Kang *et al.*, 1992; Macaya *et al.*, 1993). Although a fold-back structure has not been established for some of these (Wang *et al.*, 1991a,b), we speculate that all are forming folded structures. The unambiguously parallel G-quadruplexes that have been investigated by NMR so far all have all *anti* bases in all four strands (Aboul-ela *et al.*, 1992; Cheong & Moore, 1992; Wang & Patel, 1992).

The alternation of *syn* and *anti* bases in quadruplex DNA structures is different from that seen in Z-DNA (Wang *et al.*, 1979). In Z-DNA, the sugars of the *syn* bases flip 180° relative to the bases, resulting in the zigzag alternating phosphodiester backbone (Rich *et al.*, 1984). In the quadruplexes, the *syn* guanine bases flip relative to the sugars, so the phosphodiester backbone remains relatively B-DNA-like. The chemical shifts of the guanine phosphates in the $^{31}P$ spectrum are also consistent with a B-DNA-like phosphodiester backbone. All of the nucleotides have S-type (near C2′-*endo*) sugar puckers, in contrast to the C3′-*endo* sugar puckers of the *syn* bases in Z-DNA.

A consequence of the alternation of *syn-anti* glycosidic torsion angles along each edge of the G-quadruplex is that G-quartets alternate orientation; *i.e.*, the relative arrangement of the G-quartets is flipped 180° from one G-quartet to the next. Such a head-to-head arrangement of G-quartets was first proposed for guanosine gels by Gellert *et al.* (1962) on the basis of a 6.7-Å reflection seen by X-ray diffraction and by others (Borzo & Laszlo, 1978; Pinnavaia *et al.*, 1978; Guschlbauer *et al.*, 1990). The alternation of G-quartets also results in a change in direction of proton donors and acceptors around each G-quartet.

*Thymines Loop Diagonally across the G-Quartet at Either End of the Quadruplex.* The alternation of *syn* and *anti* guanines along the edges of the G-quadruplex results in a pattern of base–H1′,H2′,H2″ NOE cross peaks connecting 5′-*syn-anti*-3′ residues (Figure 5B and not shown), but no NOE connectivities of this kind between 5′-*anti-syn*-3′ residues. Each 5′-*syn-anti*-3′ guanine pair also has a $G_{syn}H8$–$G_{anti}H8$ cross peak, *i.e.*, $G_1$–$G_2$, $G_3$–$G_4$, $G_9$–$G_{10}$, and $G_{11}$–$G_{12}$ (Figures 5A and 7). In all of the NOESY spectra of Oxy-1.5 and derivatives, an additional H8–H8 cross peak between a *syn* G and an *anti* G *which are not sequential along the strand* is present (Figures 5A and 7). The relative locations of the H8 protons in the four possible symmetrical quadruplexes with loops at opposite ends are illustrated in Figure 10. The same *sequential syn-anti* NOE connectivities would be observed for all the structures. However, the *nonsequential* NOEs would be quite different. For each structure, there are four possible short H8–H8 distances across the grooves; however, due to symmetry, only one NOE could be observed. For the edge-looped structures, the possible nonsequential GH8–GH8 connectivities are between two *syn* Gs or two *anti* Gs. Only the two diagonally looped structures can have a nonsequential connectivity between a *syn* G and an *anti* G. Thus, even without specific assignments, the presence of a

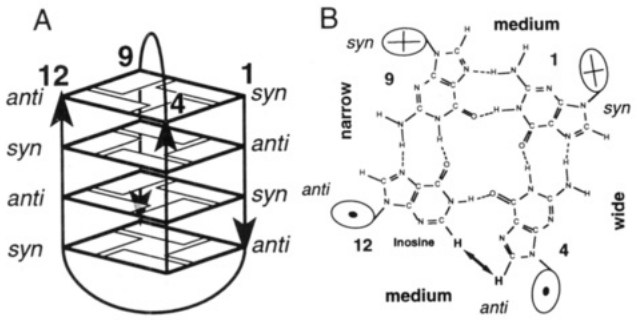


FIGURE 11: (A) Orthographic schematic of the quadruplex structure formed by Oxy-1.5 and I12. The relative locations of the bases in the end quartet are indicated. Strand direction along each edge of the quadruplex is indicated by arrows; note that there are both parallel and antiparallel strands. (B) Guanine quartet with inosine substituted at position 12. The number of the bases and glycosidic conformations for this G-quartet are indicated. The short $I_{12}H2$–$G_4H8$ interproton distance expected to give rise to an NOE is indicated by the arrow. Strand polarity is indicated by the arrow tails (crosses) and arrow heads (points) in the ellipses. The relative locations of the ribose rings due to the glycosydic torsion angle and tetrahedral C1′ are represented by the positions of the ellipses. The three different types of grooves so formed are labeled narrow, medium, and wide.

nonsequential $G_{syn}H8$–$G_{anti}H8$ NOE rules out the edge-looped quadruplex structures for Oxy-1.5 in solution.

In order to determine which diagonally looped quadruplex (A or B in Figure 10) was formed, we needed to determine whether the nonsequential $G_{syn}H8$–$G_{anti}H8$ was $G_2$–$G_{11}$ or $G_3$–$G_{10}$. From the NOESY data alone, we could assign $G_3$-H8 and $G_{11}H8$. Since the cross peak is from $G_{11}$ and not $G_3$, the structure must be structure A, as previously reported (Smith & Feigon, 1992).

Although the diagonally looped structure was initially deduced on the basis of the only ordering of guanine *syn-anti* pairs that was consistent with NOE cross peaks and intensities observed, the independent through-bond assignments obtained from the $^{31}P$–$^1H$ heteroCOSY (Figure 7) were identical to those obtained from the NOESY spectrum alone. This establishes model-independently that the nonsequential $G_{syn}H8$–$G_{anti}H8$ cross peak is between $G_2$ and $G_{11}$. The I12 derivative gives additional results that are only consistent with the diagonally looped structure of Figure 10A. The $I_{12}H2$ has an unambiguous cross peak to $G_4H8$ (Figure 7). Figure 11 illustrates the placement of bases in I12 and the residues of the G-quartet containing $I_{12}$. Only for the diagonally looped structure illustrated would there be an $I_{12}H2$–$G_4H8$ NOE cross peak. For the alternative diagonally looped structure of Figure 10B, the expected NOE would be from $I_{12}H2$ to $G_9H8$. For the two edge-looped structures (C and D), $I_{12}H2$ should be close to $G_1H8$ or $G_9H8$, respectively.

We emphasize that the specific NOE cross peaks discussed above illustrate only some of the NMR evidence which established that the quadruplexes formed by Oxy-1.5 in the solution conditions described here have loops across a specific diagonal. This model is the only one that was consistent with *all* of the NOE data; *e.g.*, no other end-looped structure was consistent with the NOE cross peaks and intensities observed for the imino resonances. Figure 12 illustrates the complexity of the network of imino–imino NOE connectivities. The odd long-range NOE connectivities (*e.g.*, $G_1$-$G_{10}$-$G_{11}$-$G_9$) are seen to fall into a neat pattern in this context. Both intra- and interquartet NOEs are observed. Interestingly, due to symmetry, some cross peaks (specifically $G_2$–$G_3$ and $G_{10}$–$G_{11}$) represent both inter- and intraquartet NOEs.

In a recent report on a closely related sequence, $d(G_3T_4G_3)$ (Scaria *et al.*, 1992), two sets of $^1H$ resonances were observed

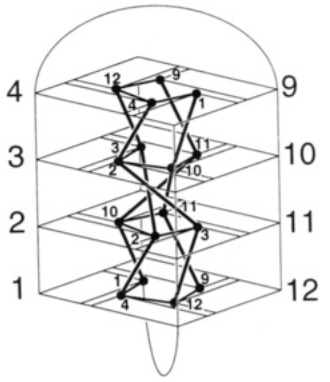


FIGURE 12: Schematic drawing of the Oxy-1.5 quadruplex structure illustrating the network of imino–imino NOEs. NOEs identified in the Oxy-1.5 and I12 spectra are included. Some missing intraquartet NOEs are expected to be small and are usually near the diagonal, so their absence is probably not significant. Both intra- and interquartet connectivities are indicated for $G_2$–$G_3$ and $G_{10}$–$G_{11}$, although only one cross peak is observed due to symmetry.

in the presence of NaCl or KCl. This evidence for an asymmetric quadruplex was taken as evidence against a diagonally looped structure. This conclusion is not justified due to the symmetry characteristics of guanine quartets. A guanine quartet, while 4-fold symmetric about the center, has two distinct faces and thus cannot be rotated (flipped) onto itself about a symmetry axis in the plane of the G-quartet. In a structure containing an even number of G-quartets, the G-quartets can be arranged so that there is a 2-fold symmetry axis between two G-quartet planes. In this way, the Oxy-1.5 structure presented here can have symmetric loops at opposite ends of a stack of G-quartets. In the $d(G_3T_4G_3)$ structure, however, there are probably an odd number of G-quartets. Any quadruplex with an odd number of G-quartets and loops at opposite ends cannot be 2-fold symmetric, since there cannot be a symmetry axis through the plane of the central G-quartet. The only possible symmetry element in an odd-numbered stack of G-quartets is along the central axis. In this case, both loops would be at one end of the stack (similar to Figure 9C,D) and might interact in a nonsymmetrical way, leading to an asymmetric complex. Thus, since all possibilities must be or could be asymmetric, no structural conclusions about strand orientation can be drawn from the data presented by Scaria *et al.* (1992).

The diagonally looped Oxy-1.5 quadruplex requires that formation of the quadruplex occur by some mechanism other than simple dimerization of two preformed hairpin monomers with the same hydrogen bonding between G·G pairs as found in G-quartets. We have seen no evidence for any monomeric structures; *i.e.*, no evidence for alternative hydrogen-bonded conformations is observed in the NMR spectra even at temperatures where the quadruplex starts to melt ($T_m \sim 67$ °C).

*Adjacent Strands of Oxy-1.5 Are Parallel and Antiparallel.* An important consequence of the diagonal looping of the thymines across the G-quartets is that, in contrast to edge-looped structures, adjacent strands are not all antiparallel. Instead there are two pairs of parallel strands and two pairs of antiparallel strands, as illustrated in Figure 11. The glycosidic torsion angles *around* each G-quartet are *syn-syn-anti-anti* (Figure 11B). Antiparallel strands have hydrogen bonds between guanines with different glycosidic torsion angles (*syn-anti* or *anti-syn*), and parallel strands have hydrogen bonds between guanines with the same glycosidic torsion angle (*syn-syn* or *anti-anti*).

NOESY spectra of the inosine derivative (I12) prove directly that parallel strands are present in the Oxy-1.5 structure. Inosine 12, which is in the *anti* conformation (G12 in Figure 5B), has an NOE cross peak between the $I_{12}$H2 and the $G_4$-H8, which is also an *anti* nucleotide. This unambiguously places two *anti* nucleotides next to each other in the end G-quartet.

A recent study by Kallenbach and co-workers (Lu *et al.*, 1993) indicates that an all-parallel dimeric quadruplex formed by d($G_4T_25'$–$5'T_2G_4$) is more thermodynamically stable than that formed by d($G_4T_4G_4$). The partial parallel character of the diagonally looped structure may explain why this structure is favored in solution over the all-antiparallel structure observed in the crystal (Kang *et al.*, 1992).

*Oxy-1.5 Has Three Different Groove Widths.* Each of the four grooves in the quadruplex has the same pattern of base proton donors and acceptors due to the 4-fold symmetry of the G-quartets. The approximate locations of the guanine base atoms are similar in all four grooves. Thus, the four grooves in the quadruplex are only distinguished by the positions of the backbone atoms. Each deoxyribose ring is tilted toward one side of the glycosydic bond due to the tetrahedral bonding of the C1′ atom. This results in three different groove widths (Figure 11B). The narrow groove is formed between two antiparallel strands where the sugars are tilted toward each other. The wide groove is formed between antiparallel strands where the sugar rings tilt away from each other. The two symmetry-related medium grooves are formed between the parallel strands where both sugar rings are tilted in the same direction. Because the orientation of the guanines is similar in each of the grooves, the pattern of potential base hydrogen-bond donors and acceptors varies only in their accessibility.

*Imino and Amino Protons of Oxy-1.5 Are Unusually Slowly Exchanging.* An interesting feature of these molecules is the extremely long-lived (slowly exchanging) imino and amino resonances. Four of the imino resonances, which correspond to imino protons from the central two G-quartets, are still observable more than 2 weeks after transfer of the sample from $H_2O$ to $D_2O$. The exhange behavior of the amino protons is also unusual. In B-DNA, the hydrogen-bonded and non-hydrogen-bonded guanine amino protons exchange with each other as well as with water. This generally leads to observation of only one broad amino resonance for the G amino pair in $H_2O$ spectra (Boelens *et al.*, 1985). In the Oxy-1.5 and I12 spectra, however, four of the amino groups are observed as sharp, well-resolved resonance pairs in $H_2O$. Two of these amino protons pairs, corresponding to the central two *syn* guanines ($G_3$ and $G_{11}$), are still observed up to several days after transfer of the sample from $H_2O$ to $D_2O$. Thus, neither the hydrogen-bonded nor the non-hydrogen-bonded amino proton on these nucleotides exchanges over a period of days.

Slowly exchanging imino resonances have also been reported for parallel quadruplex structures (Cheong & Moore, 1992; Wang & Patel, 1992). This indicates that the G-quartet structure itself leads to a very slow exchange rate, perhaps by exclusion of solvent from the center of the quadruplex. However, the iminos in these other quadruplexes exchange on the order of days and not the weeks observed for Oxy-1.5. The slower exchange rates of the imino and amino protons of Oxy-1.5 can be rationalized by the diagonally looped quadruplex structure. An edge-looped quadruplex can dissociate by separation of two hairpins, so only 16 hydrogen bonds need to be broken. In the tetrameric parallel structures, one strand can dissociate at a time. In contrast, for the diagonally looped structure, all 32 hydrogen bonds must be broken for the quadruplex to come apart.

*Cation Dependence of Oxy-1.5 Structures.* The NMR spectra of Oxy-1.5 in both 50 mM NaCl and 50 mM KCl indicate that although there are some conformational differences between the quadruplexes formed with the two cations, they are both qualitatively the same diagonally looped structure. The samples of Oxy-1.5 prepared with KCl have the very high melting points reported for $K^+$-stabilized quadruplexes (>90 °C) (Guschlbauer *et al.*, 1990), effectively preventing thermal melting of the two DNA strands of the quadruplex. Nevertheless, it is possible to substitute $Na^+$ for $K^+$ and vice versa simply by passing the DNA over a cation-exchange column. Addition of only a small amount of KCl to a sample in 50 mM NaCl will convert the sample to the conformation observed in KCl alone. These observations suggest that the conformational differences between Oxy-1.5 in NaCl and Oxy-1.5 in KCl are induced by cation binding without disruption of the folded structure. The quantitative differences between the conformations with the two different cations will be the subject of future investigations.

*Comparison of Solution and Crystal Structures of Oxy-1.5.* The recently reported crystal structure of Oxy-1.5 (Kang *et al.*, 1992) and the solution structure of Oxy-1.5 show several features in common. Both form dimeric quadruplexes with thymine loops at opposite ends. The nucleotides in both structures have alternating *syn* and *anti* glycosidic torsion angles along each edge of the quadruplex. The major difference between the two structures is in the orientation of the loops. In the crystal structure, the thymine loops go across an edge of the G-quartets, spanning the wide groove (Figure 11C). Thus, all strands in the crystal structure are antiparallel and the nucleotides in each G-quartet are *syn-anti-syn-anti*. There are only two types of grooves, two wide grooves and two narrow grooves.

The different crystal and solution structures can perhaps be rationalized, since there is evidence that these types of oligonucleotides can form multiple different structures depending on the salt conditions and how the sample was prepared (Sen & Gilbert, 1990; Williamson *et al.*, 1989). In our solution NMR samples, there is usually evidence for some larger or aggregated complexes, in addition to the differences observed in NaCl and KCl. One possible explanation for the difference between the solution and crystal structures might have been the different cation used in preparing the samples; *i.e.*, the major counterion for the crystal samples was $K^+$, while for our solution sample the counterion was $Na^+$. However, as discussed above, in solution Oxy-1.5 forms a diagonally looped structure in both NaCl and KCl. In fact, the sample used in our original study (Smith & Feigon, 1992) had about 10 mM KCl (impurity) in addition to the NaCl. Thus, the difference in $K^+$ *vs* $Na^+$ counterion cannot simply explain the different structures obtained. It is possible that differences in sample preparation and the presence of other counterions, *e.g.*, spermine and $Mg^{2+}$ used in the crystallization liquor, might favor the edge-looped structure found in the crystal over the diagonally looped structure found in our solution conditions.

Different crystal and solution structures of the same oligonucleotide are not unprecedented. Many DNA oligonucleotides crystallize in the A-DNA conformation (Dickerson, 1992) yet give NMR spectra indicative of a B-DNA conformation in solution. DNA sequences with alternating C-G sequences only crystallize as Z-DNA (Rich *et al.*, 1984)

yet appear as Z-DNA in solution only under very high salt or dehydrating conditions and are otherwise B-DNA. An RNA oligonucleotide which forms only a hairpin in solution (Cheong *et al.*, 1990) was recently crystallized and found to form a mismatched duplex in the crystal (Holbrook *et al.*, 1991).

*Three-Dimensional Structure of Oxy-1.5.* The well-resolved NOESY (Figure 3) and COSY spectra (not shown) of Oxy-1.5 allow for accurate cross-peak integration of NOE cross peaks and accurate determination of *J*-coupling constants. These data are currently being incorporated into a metric matrix distance geometry algorithm to generate a complete three-dimensional structure of Oxy-1.5 (manuscript in preparation). A comparison of the structures of Oxy-1.5 and Oxy-3.5 will also be presented elsewhere.

## ACKNOWLEDGMENT

The authors thank Karl Koshlap and Shiva Malek for synthesis of the DNA and Edmond Wang and Dara Gilbert for many helpful discussions about symmetry and NMR.

## REFERENCES

Aboul-ela, F., Murchie, A. I. H., & Lilley, D. M. J. (1992) *Nature 360*, 280–282.
Acevedo, O. L., Dickinson, L. A., Macke, T. J., & Thomas, C. A., Jr. (1991) *Nucleic Acids Res. 19*, 3409–3419.
Altona, C. (1982) *Recl. Trav. Chim. Pays-Bas 101*, 413–433.
Arnott, S., & Selsing, E. (1974) *J. Mol. Biol. 108*, 551–552.
Arnott, S., Chandrasekaran, R., & Marttila, C. M. (1974) *Biochem. J. 141*, 537–543.
Balagurumoorthy, P., Brahmachari, S. K., Mohanty, D., Bansal, M., & Sasisekharan, V. (1992) *Nucleic Acids Res. 20*, 4061–4067.
Bax, A., & Davis, D. G. (1985) *J. Magn. Reson. 65*, 355–360.
Blackburn, E. H., & Gall, J. G. (1978) *Proc. Natl. Acad. Sci. U.S.A. 78*, 2263–2267.
Boelens, R., Scheek, R. M., Dijkstra, K., & Kaptein, R. (1985) *J. Magn. Reson. 62*, 378–386.
Borzo, M., & Laszlo, P. (1978) *C.R. Acad. Sci. Paris 287*, 475–478.
Chantot, J. F., & Guschlbauer, W. (1969) *FEBS Lett. 4*, 173.
Chen, F.-M. (1992) *Biochemistry 31*, 3769–3776.
Cheong, C., & Moore, P. B. (1992) *Biochemistry 31*, 8406–8414.
Cheong, C., Varani, G., & Tinoco, I., Jr. (1990) *Nature 346*, 680–682.
de Leeuw, F. A. A. M., & Altona, C. (1983) *J. Comput. Chem. 4*, 428–437.
Feigon, J., Leupin, W., Denny, W. A., & Kearns, D. R. (1983) *Biochemistry 22*, 5943–5951.
Gellert, M., Lipsett, M. N. & Davies, D. R. (1962) *Proc. Natl. Acad. Sci. U.S.A. 48*, 2013–2018.
Guschlbauer, W., Chantot, J.-F., & Thiele, D. (1990) *J. Biomol. Struct. Dyn. 8*, 491–511.
Hardin, C. C., Henderson, E., Watson, T., & Prosser, J. K. (1991) *Biochemistry 30*, 4460–4472.
Hare, D. R., Wemmer, D. E., Chou, S. H., Drobny, G., & Reid, B. R. (1983) *J. Mol. Biol. 171*, 319–336.
Henderson, E., Hardin, C. C., Walk, S. K., Tinoco, I., Jr., & Blackburn, E. H. (1987) *Cell 51*, 899–908.
Holbrook, S. R., Cheong, C., Tinoco, I., Jr., & Kim, S.-H. (1991) *Nature 353*, 579–581.
Jin, R., Breslauer, K. J., Jones, R. A., & Gaffney, B. L. (1990) *Science 250*, 543–546.
Jin, R., Gaffney, B. L., Wang, C., Jones, R. A., & Breslauer, K. J. (1992) *Proc. Natl. Acad. Sci. U.S.A. 89*, 8832–8836.
Kang, C., Zhang, X., Ratliff, R., Moyzis, R., & Rich, A. (1992) *Nature 356*, 126–131.
Kintanar, A., Klevit, R. E., & Reid, B. R. (1987) *Nucleic Acids Res. 15*, 5845–5862.
Klobutcher, L. A., Swanton, M. T., Domini, P., & Prescott, D. M. (1981) *Proc. Natl. Acad. Sci. U.S.A. 78*, 3015.
Kumar, A., Ernst, R. R., & Wüthrich, K. (1980) *Biochem. Biophys. Res. Commun. 95*, 1–6.
Lu, M., Guo, Q., & Kallenbach, N. R. (1992) *Biochemistry 31*, 2455–2459.
Lu, M., Guo, Q., & Kallenbach, N. R. (1993) *Biochemistry 32*, 598–601.
Macaya, R. F., Schultze, P., & Feigon, J. (1992) *J. Am. Chem. Soc. 114*, 781–783.
Macaya, R. F., Schultze, P., Smith, F. W., Roe, J. A., & Feigon, J. (1993) *Proc. Natl. Acad. Sci. U.S.A. 90*, 3745–3749.
Marion, D., & Bax, A. (1988) *J. Magn. Reson. 80*, 528–533.
Marion, D., Ikura, M., & Bax, A. (1989) *J. Magn. Reson. 84*, 425–430.
Murchie, A. I. H., & Lilley, D. M. J. (1992) *Nucleic Acids Res. 20*, 49–53.
Oka, Y., & Thomas, C. A., Jr. (1987) *Nucleic Acids Res. 15*, 8877–8898.
Panyutin, I. G., Kovalsky, O. I., Budowksy, E. I., Dickerson, R. E., Rikhirev, M. E., & Lipanov, A. A. (1990) *Proc. Natl. Acad. Sci. U.S.A. 87*, 867–870.
Pardi, A., Walker, R., Rapoport, H., Wider, G., & Wüthrich, K. (1983) *J. Am. Chem. Soc. 105*, 1562–1653.
Pinnavaia, T. J., Marshall, C. L., Metterl, C. M., Fisk, C. L., Miles, T., & Becker, E. D. (1978) *J. Am. Chem. Soc. 100*, 3625–3627.
Rich, A., Nordheim, A., & Wang, A. H.-J. (1984) *Annu. Rev. Biochem. 53*, 791–846.
Scaria, P. V., Shire, S. J., & Shafer, R. H. (1992) *Proc. Natl. Acad. Sci. U.S.A. 89*, 10336–10340.
Scheek, R. M., Russo, N., Boelens, R., & Kaptein, R. (1983) *J. Am. Chem. Soc. 105*, 2914–2916.
Sen, D., & Gilbert, W. (1988) *Nature 334*, 364–366.
Sen, D., & Gilbert, W. (1990) *Nature 344*, 410–414.
Sklenář, V., & Bax, A. (1987) *J. Magn. Reson. 74*, 469–479.
Sklenář, V., Miyashiro, H., Zon, G., Miles, H. T., & Bax, A. (1986) *FEBS Lett. 208*, 94–98.
Smith, F. W., & Feigon, J. (1991) *J. Biomol. Struct. Dyn. 8*, 201.
Smith, F. W., & Feigon, J. (1992) *Nature 356*, 164–168.
Smith, S. S., Baker, D. J., & Jardines, L. A. (1989) *Biochem. Biophys. Res. Commun. 160*, 1397–1402.
States, D. J., Haberkorn, R. A., & Ruben, D. J. (1982) *J. Magn. Reson. 48*, 286–292.
Sundquist, W. I., & Klug, A. (1989) *Nature 342*, 825–829.
Wang, A. H.-J., Quigley, G. J., Kolpak, F. J., Crawford, J. L., van Boom, J. H., van der Marel, G., & Rich, A. (1979) *Nature 282*, 680–686.
Wang, K. Y., McCurdy, S., Shea, R. G., Swaminathan, S., & Bolton, P. H. (1993) *Biochemistry 32*, 1899–1904.
Wang, Y., & Patel, D. J. (1992) *Biochemistry 31*, 8112–8119.
Wang, Y., de los Santos, C., Gao, X., Greene, K., Live, D., & Patel, D. J. (1991a) *J. Mol. Biol. 222*, 819–832.
Wang, Y., Jin, R., Gaffney, B., Jones, R. A., & Breslauer, K. J. (1991b) *Nucleic Acids Res. 19*, 4619–4622.
Weisz, K., Shafer, R. H., Egan, W., & James, T. L. (1992) *Biochemistry 31*, 7477–7487.
Williamson, J. R., Raghuraman, M. K., & Cech, T. R. (1989) *Cell 59*, 871–880.
Zahler, A. M., Williamson, J. R., Cech, T. R., & Prescott, D. M. (1991) *Nature 350*, 718–720.
Zakian, V. A. (1989) *Annu. Rev. Genet. 23*, 579–604.
Zimmerman, S. B., Cohen, G. H., & Davies, D. R. (1975) *J. Mol. Biol. 92*, 181–192.